Raw water lily leaves (*nymphaea lotus*) powder as an effective adsorbent for the adsorption of malachite green dye from aqueous solution.

Hamisu Abdulmumini [a], Abdullahi Muhammad Ayuba [b]*

aDepartment of Science Laboratory Technology, Scholl of Scienec and Technology, Abubakar Tatari Ali Polytechnic, PMB 0094, Bauchi, Nigeria
bDepartment of Pure and Industrial Chemistry, Bayero University, PMB 3011, Kano, Nigeria

ARTICLE INFO

ABSTRACT

In this present study, raw water lily leaves (RWL) powder was prepared and used as low cost, efficient and environmental friendly adsorbent for the removal of malachite green (MG) from aqueous solution. The adsorbent's surface functional group, net neutral charge and morphology were analysed by FT-IR, Point of Zero charge and Scanning Electron (SEM) spectroscopic techniques which confirmed the effective adsorption of MG dyes onto the RWL adsorbent surface. Batch adsorption technique was employed under various optimized conditions including contact time, adsorbent dosage, adsorbate concentration, pH and temperature respectively with an adsorption capacity of 216.66mg/g and percentage adsorption of 99.5. The physical properties: moisture content (13.49%), ash content (9.81%), organic matter (90.19%), bulk density (0.263g/cm^3), pore volume (1.66cm^3), pH (5.74) of the adsorbent were obtained using standard methods. The kinetic data were best fitted by pseudo-second order in all the models tested under different operating temperatures. The adsorption isotherms were estimated, established and found to fit into Freundlich isotherm as compared to other models tested. Thermodynamics of the adsorption was found to be spontaneous and feasible with values of Gibb's free energy (ΔG) ranging between -9.481 to -9.880kJ/mol, exothermic with enthalpy (ΔH) of -11.75kJ/mol and a decrease in randomness of the adsorption process during the transfer of molecules between the adsorbent and adsorbates with entropy (ΔS) of -6.33kJ/mol. This study confirmed that RWL could be employed as a low cost and environmental friendly adsorbent for the removal of toxic dyes such as Malachite Green from aqueous solution.

1. Introduction

Textile, paper, printing and dye industries consume large quantities of water at different stages of dyeing and finishing processes [1]. The contamination of drinking water by dyes at even minute concentration could significantly impact on its colour making it unfit for human consumption [2] as these dyes are non-biodegradable, highly toxic, carcinogenic and mutagenic pollutants [3].

Malachite green (MG), a cationic, water soluble organic dye is a member of the triphenylmethane family [4]. Its employed in variety of substrate materials including wool, textile, paper, leather, cotton, and acyrilics fibres in silk, textile and jute industries [5].

Also, it is used as colorants [6], biocide in agricultural industries [7], therapeutic agent, anthelminthic and medical disinfectant [8]. Despite its wide range of applications, reports describe it as carcinogenic, hazardous, tumour promoting agent in mammalian liver cell [9]. Therefore, present of MG in drinking water, foodstuff, fishes and animal milk used by human is of great concern [10].

A variety of methods have been employed for removal of dyes from coloured effluents such as membrane filtration, oxidation, coagulation-flocculation, biological treatment, electrochemical processes and adsorption [11-13]. However, these methods have shown their limit especially with regards to the rate of removal of the pollutants and the cost of their

---

* Corresponding author. Tel.: +2348062771500; e-mail: ayubaabdullahi@buk.edu.ng

application [14]. In contrast, adsorption is more suitable and prime for treatment method, due to its simplicity of design, ease of operation, high efficiency and cost effectiveness [15]. Initially, literature reported activated carbon is the most widely used adsorbent [16]. However, due to high cost of activated carbon, many researchers has explored the feasibility of using available waste bio-materials as its possible replacements. Bio-sorption based on binding capacities of different low cost adsorbents such as natural, agricultural and industrial by-product waste are attractive because of their abundant availability at low or no cost, good performance of removing dyes from aqueous solutions and minimum volume of sludge generated for disposal [17-18].

Adsorbents of plants origin were reported to have been investigated by many researchers for carcinogenic dyes removal from waste water such Bambara groundnut hull [1, 19], desert date seed shell activated carbon [20], jackfruit [21], corn cob [22], Verdc hull [23], *Balamite aegyptiaca* [24] among others. In this present study, raw water Lily (RWL) leaves powder was used to remove MG from synthetic aqueous solutions. The effects of various parameters such as contact time, adsorbents dosage, initial concentration, pH of the solution and temperature on the adsorption efficiency of MG were studied using batch experimental techniques. Thermodynamic and kinetic parameters for MG adsorption onto RWL adsorbent was analysed in addition to isotherm models to propose suitable mechanism for the adsorption process

2. Results and Discussion
2.1 The physicochemical analysis of the adsorbents
The physical parameters of the adsorbents are presented in Table 1. The sample were found to be rich in moisture and organic matter. The pH was found to be 5.74 which is relatively lower than 6 - 8 acceptable pH for most applications adsorbent as reported by Bello *et al*. [34]. The ash content value obtained in this research is 9.81 which indicates good amount of residue (inorganic matter) or minerals such as sodium, magnesium, calcium etc in pores of the adsorbent [35]. The bulk density and pore volume are also important physical parameters, because they have been reported to enhanced adsorption capacity of adsorbents to a large extent. The bulk density recorded in this study (0.263gm/ml ±0.01) is higher than that reported (0.21g/ml±0.02) by Ravichandran [36].

Table 1: The physical properties of the prepared adsorbent (RWL)

| Parameters	Values
Moisture(%)	13.49±0.23
Ash (%)	9.81±0.37
Organic Matter (%)	90.19±0.37
pH	5.74±0.12

Pore volume (cm³)	1.66±0.13
Density (g/cm³)	0.263±0.12

2.2 Characterization of the Adsorbent
FT-IR analysis
In the FT-IR spectrum shown in fig 1 of RWL before and after adsorption. There were notable changes in absorption band and peaks after the adsorption of MG dye onto the adsorbent. The notable peaks observed are hydroxyl group (-OH), -CH stretch, carboxylic groups, C=C group, aromatic rings, C-O stretch and C-H aromatic were all present after adsorption with little changes. However, the shift in bands and wavenumbers between before and after adsorption of the samples as shown in table 2 can be predicted to signify vander Waals interaction during adsorption process. However, participation of both functional groups from the dye and adsorbent is an established phenomenon during adsorption as reported by Karim *et al.* [37] and Parhi *et al.* [38] among others.
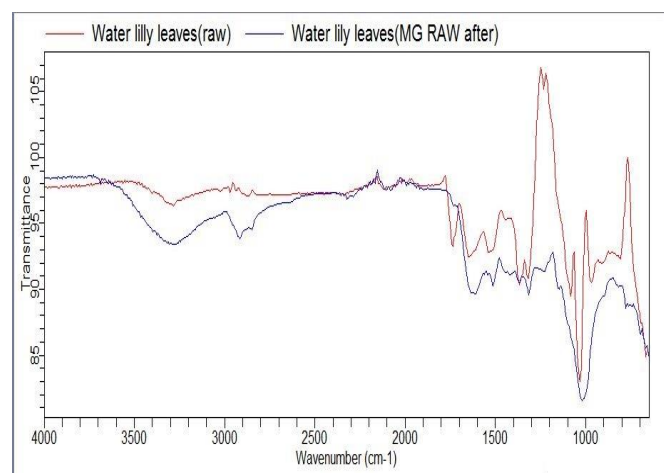

Fig 1. FT-IR Spectra for Adsorption of MG dye onto RWL before and After adsorption

Table 2. Different functional groups recognized before and after adsorption of MG onto RWL adsorbent.

Functional group	Wavelength range (cm⁻¹)	Malachite Green (MG)		
		Before Adsorption	After Adsorption	Difference
O-H stretch	3300-3400	3444	3309	135
C-H stretch	2950-2800	2950	2918	32
C≡C alkynes	2100-2260	2119	2106	13
COOH group	1690-1760	1632	1614	18
C=C aromatics	1500-1700	1405	1514	109
C-O stretch	1080-1300	-	1316	1316
C-H Aromatic	675- 1050	1080	1022	58

SEM Spectroscopy

Scanned micrographs of the RWL adsorbent before and after adsorption of MG were taken at an accelerating voltage of 15kV and 1500X magnifications. The SEM before adsorption fig 3(a) shows a pores spongy like surface while the micrograph of RWL adsorbent after adsorption of MG dye fig 3b shows deposition of dye molecules onto the surface of the adsorbent result in formation of a heterogeneous surface with filled cracks, pores and rough surfaces. This shows an evidence of interactions between the dyes and the adsorbent surface.
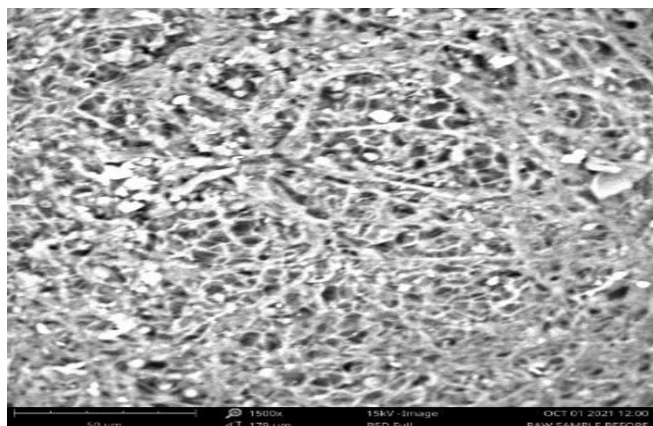

(a)
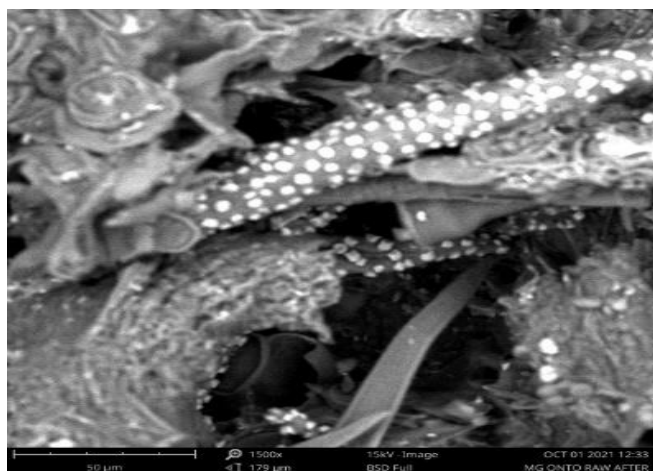
(b)

Fig 3(a). SEM micrograph for Raw sample before adsorption **(b).** SEM of MG onto RWL after adsorption.

Point of zero charge

The point of zero charge (PZC) is the pH at which the surface of the adsorbent has net neutral charge. Fig 4 shows result of PZC of RWL adsorbent. As shown the point in the figure, the PZC of RWL adsorbent is 5.40. This implies that at the pH below 5.40, the surface charge of the adsorbent is positive while at pH above 5.40 the surface charge of the adsorbent is negative [39]. This study result is higher than reported by Akinlola and Umar of 3.50 [40] and 3.00 for groundnut shell and beans pod respectively and

lower than 6.00 for watermelon shell reported by Zhang *et al*. [41].
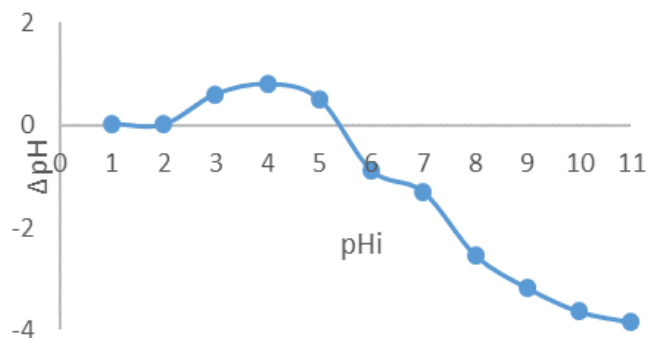
Fig 4. Point of zero Charge for the RWL adsorbent

2.3 Batch adsorption experiment and optimization

Fig 5(a) indicates the effect of contact time on adsorption of MG onto RWL adsorbent by varying from 5-120 minutes at room temperature and initial concentration of 100mg/L. The dyes uptake was very fast initially for the first 15minutes. It's slow down as the surface of RWL become saturated with MG and eventually reaches maximum after 90 minutes and the agitation time was therefore set at 90 minutes as optimal contact time.

Fig 5(b) shows effect of the quantity of RWL used for the adsorption of MG in which amount of adsorbent was varied from 20-200mg while other operating conditions was kept constant. It was observed that adsorption capacity of the adsorbents decreases with increasing dosage probably due limited contact or inaccessibility of the active sites. Similarly, % removal increases with increasing dosage. Similar trends were reported by Bedmohata *et al.* [42], Liu *et al.* [43] and Yusuf *et al.* [44].

Fig 5(c) indicates the effect of initial concentration of MG onto RWL by varying the initial concentration from 20-10mg/L. The adsorption capacity increases with increasing initial concentration probably due to high driving forces to overcome mass transfer resistance [45], thereby enhancing interaction between the adsorbent and the adsorbate and hence resulting in high dyes update from 45.21mg/g at 20mg/L to 276.08mg/g at 120 mg/L respectively [46]. While percentage removal increases progressively from low concentration until it reached an optimum value and then decrease as the concentration increases. This is partly due the fact that the vacant site or active site of the adsorbent become saturated or inaccessible by the adsorbent at higher concentrations.

Fig 5(d) indicates the effect of pH on adsorption of MG onto RWL adsorbent surface. pH of a solution plays an important role in the whole adsorption process particularly on adsorption capacity [1]. MG being cationic dye gives positive charge when dissolves in water. In acidic medium, the positive charge on the surface of the adsorbents tend to compete or repel the

excess H⁺ ions in the adsorption of MG at pH<7 which result in low adsorption of the dye molecules at low pH. However, there is significant increase in MG adsorption when the pH of the dye solution was increased (pH>7) implying that the process is probably or solely electrostatic interaction. Similar trends were reported by other researchers [47-50].

(a)

(b)

(c)

(d)

Fig 5: Effect of (a) Contact time (b) Dosage on adsorption of MG onto RWL adsorbent (c) Initial Concentration (d) pH on adsorption of MG onto RWL adsorbent

2.4 Adsorption kinetics studies

The study of adsorption kinetics of MG onto RWL could provide an important information on the adsorption rate and the factors affecting it. For this study, contact time of adsorption was varied from 5 to 60 minutes with interval of 5 minutes where by operating parameters were kept at optimized condition at temperature of 30, 40, 50⁰C respectively. Pseudo first order, pseudo second order, Elovich and intra-particle diffusion models were employed to analyse the kinetic of MG onto the RWL adsorbents:

Pseudo first order kinetic model

The pseudo first order equation used is usually express according to equation (1) [51]:

$$\frac{dq_t}{dt} = k_1(q_e - q_t)\dots\dots\dots\dots\dots\dots\dots (1)$$

Where q_e and q_t are amount adsorbed per unit weight of the adsorbent at equilibrium and time t respectively (mg/g), k_1 is the rate constant of pseudo first order sorption (min⁻¹). Given a boundary condition for t =0 and qt =0 the equation (1) can be integrated to give equation (2);

$$\log(q_e - q_t) = \log(q_e) - \frac{k_1 t}{2.303} \dots\dots\dots\dots(2)$$

The plot $\log(q_e - q_t)$ vs t gave a linear relationship from which k_1 and q_e were determined from the slope and intercept of fig 6(a) respectively.

Pseudo-second kinetic models

The pseudo second order adsorption kinetic rate equation is expressed as shown in equation (3):

$$\frac{dq_t}{dt} = k_2(q_e - q_t)^2 \dots\dots\dots\dots\dots\dots (3)$$

Where k_2 is the rate constant of pseudo second order adsorption (g/mg.min). Applying the boundary conditions t = 0 to t = t and $q_t = 0$ to $q_t = q_t$ the integrated form of equation (3) becomes;

$$\frac{1}{(q_e - q_t)} = \frac{1}{q_e} + k_2 t \dots\dots\dots\dots\dots\dots (4)$$

This equation can be rearranged to obtained equation (5)

$$\frac{1}{q_t} = \frac{1}{k_2 q_e^2} + \frac{t}{q_e} \dots\dots\dots\dots\dots\dots\dots(5)$$

If the initial adsorption rate, h (mg/g.min)

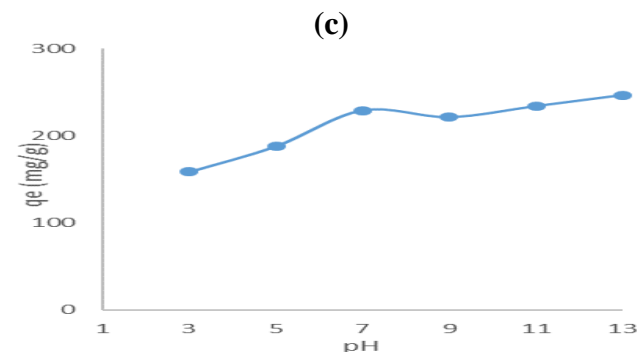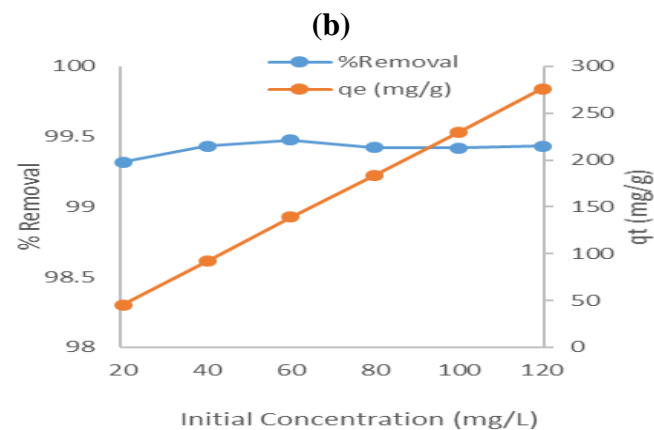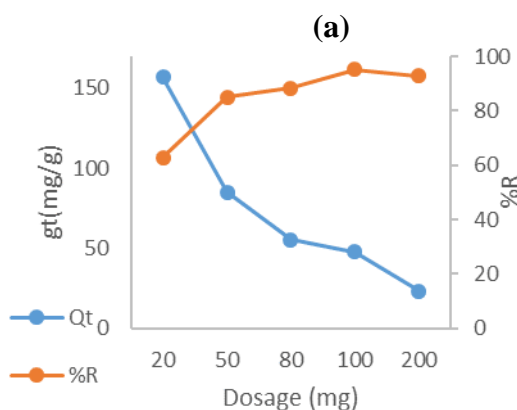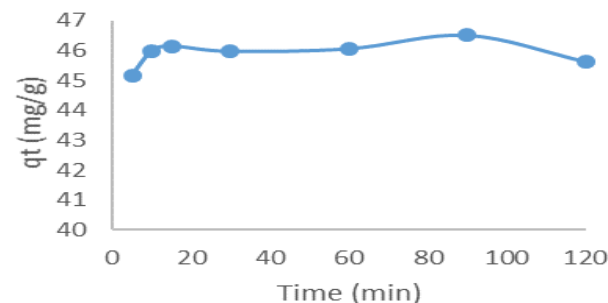$$h = k_2 q_e^2 \dots\dots\dots\dots\dots\dots\dots\dots\dots (6)$$

the equation (6) becomes;

$$\frac{t}{q_e} = \frac{1}{h} + \frac{1}{q_e}(t) \dots\dots\dots\dots\dots\dots\dots (7)$$

The plot of t/qe vs t gave a linear relationship for which q_e and k_2 were determine from the slope and intercept in figure 6(b) respectively.

Elovich Models

The Elovich kinetic model is described by equation (8);

$$q_t = \frac{1}{\beta}\ln(\alpha\beta) + \frac{1}{\beta}\ln t \quad\ldots\ldots\ldots\ldots\ldots\ldots\ldots(8)$$

This model gives useful information on the extent of both surface activity and activation energy for adsorption process. The parameters (α) and (β) was calculated from the slope and intercept of the linear plot of q_t vs ln(t) in figure 6(c).
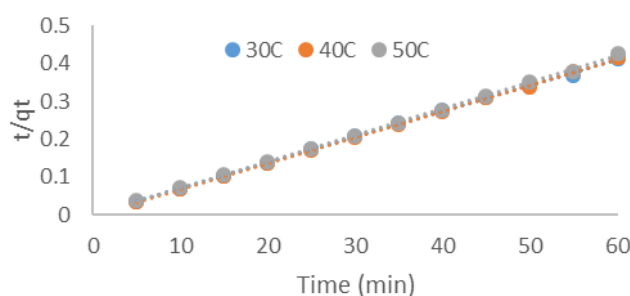
Intraparticle Diffusion model

The slowest step in an adsorption process is usually taken as the rate determining step. This step is often attributed to pore and intraparticle diffusion. Since pseudo first and second models cannot provide information on effect of intra particle diffusion in adsorption model can be used. Possibility of involvement of intra particle diffusion model as the sole mechanism was investigated according to Weber-Morris equation (9)

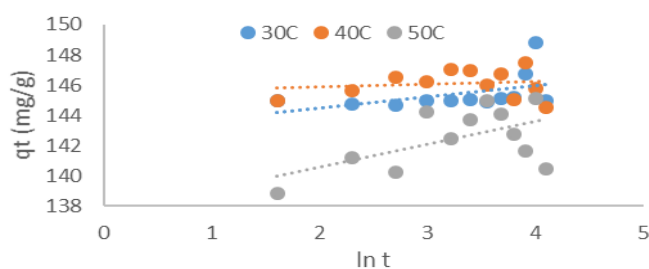$$q_t = C + k_{int}t^{1/2} \quad\ldots\ldots\ldots\ldots\ldots\ldots\ldots (9)$$

Where the constant k_{int} (mg/g.min) is the intra particle diffusion rate and C is the boundary layer thickness. If the rate limiting step is only due to intra particle diffusion, then q_t vs $t^{1/2}$ gave a linear plot which passes through the origin as shown in fig 6(d)
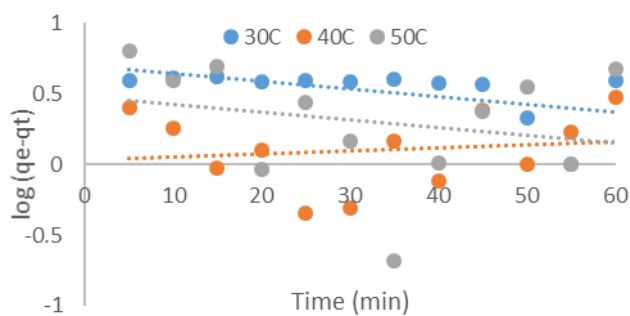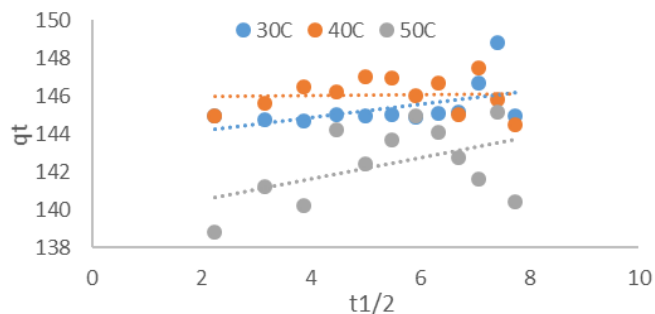
(a)

(b)

(c)

(d)

Fig 6: (a) pseudo first order **(b)** pseudo second order **(c)** Elovich model **(d)** Intraparticle diffusion model

Table 3: Calculated kinetic parameters for adsorption of MG onto RWL

Kinetic Model		Parameters			
Pseudo-First Order		q_{exp} (mg/g)	q_{cal} (mg/g)	$k_1(min^{-1})$	R^2
	30^0C	246.52	1.04	6.91×10^{-4}	0.0010
	40^0C	224.88	0.751	3.09×10^{-2}	0.6364
	50^0C	243.97	1.820	1.39×10^{-2}	0.2416
Pseudo-Second Order		q_{exp} (mg/g)	q_{cal} (mg/g)	k_2(g/mg. min)	R^2
	30^0C	246.52	243.90	1.68×10^{-1}	0.9956
	40^0C	244.88	238.10	1.47×10^{-2}	0.9998
	50^0C	243.97	238.10	1.36×10^{-2}	0.9997
Elovich Model			B	A	R^2
	30^0C		2.484	0.4032	0.2206
	40^0C		-0.627	-1.585	0.4059
	50^0C		-0.682	-1.458	0.2194
Intraparticle Diffusio			C	K_{int}	R^2
	30^0C		244.32	0.1724	0.2159
	40^0C		246.66	-0.7605	0.4922
	50^0C		243.89	-0.7123	0.2766

The kinetic parameters show in table 3 for the adsorption of MG onto RWL adsorbent indicated that the kinetic data fitted the pseudo-second order model. The R^2 values at all experimental temperatures were close to unity. The experimental and calculated adsorption capacities are in good agreement while other models tested R^2 are very low and q_{exp} and q_{cal} are quite divergent. This confirmed the applicability of the pseudo-second order kinetic model to describe the adsorption of MG onto RWL adsorbents in aqueous medium.

2.5 Adsorption Equilibrium

Adsorption isotherm models are fundamentals to describing the behaviour of adsorbent-adsorbate interaction and also for investigating the mechanism of adsorption [52]. In this study, equilibrium data was analysed using Langmuir, Freundlich, Temkin and D-R isotherm models:

Langmuir Isotherm

This model describes the homogenous adsorption of the single layer adsorbate at the adsorbent surface and is described by the linear equation (10) [53].

$$\frac{1}{q_e} = \frac{1}{q_0} + \frac{1}{q_0 K_L C_e} \quad \cdots\cdots\cdots\cdots\cdots\cdots\cdots (10)$$

Where, q_e is the amount of MG adsorbed at equilibrium (mg/g), q_0 is the monolayer adsorption capacity (mg/g) and K_L (mg/g) is expressed as the Langmuir constant associated with the coefficient of adsorption and energy of adsorption. However, q_0 and K_L were calculated using slope and intercept of a graph of $1/q_e$ against $1/C_e$ respectively and parameters reported in table 4.

To determine whether the adsorption process is favourable, a dimensionless constant separation factor R_L is defined based on equation (11) [52]:

$$R_L = \frac{1}{1 + K_L C_0} \quad \cdots\cdots\cdots\cdots\cdots\cdots\cdots (11)$$

The adsorption process is irreversible when R_L is 0.00, favourable when R_L is between 0.0 and 1.0, linear when R_L is equal to 1.0 and unfavourable when R_L is greater than 1.0. q_0, K_1, R_L and R^2.

Fruendlich Isotherm

The Freundlich model describes that adsorption is irreversible and non-ideal and the heat of distribution during adsorption process on the heterogeneous surface of the adsorbates [54]. The model is expressed using equation (12):

$$log q_e = log K_F + \frac{1}{n} log C_e \quad \cdots\cdots\cdots\cdots (12)$$

Where K_F is the Freundlich constant demonstrating the multilayer adsorption capacity and n indicates the adsorption intensity and binding energy. The values of K_F and n can be determined using intercept and slope from the plot of log qe against log Ce respectively. If n=1 then the partition between the two phase are independent of the dyes concentration. If the values of 1/n are less than 1 it indicates normal adsorption process whereas the value of 1/n is greater than 1 its indicates cooperative adsorption process. The heterogeneity parameter is indicating by value of 1/n. The smaller 1/n, the greater the heterogeneity. If n lies between 1 to 10 it indicates a favourable adsorption process. The K_F, 1/n are computed from the plot of log q_e against log C_e and reported in table 3.

D-R isotherm

This model is used to determine the adsorption behaviour of MG towards the adsorbent RWL using equation (13) [55]:

$$ln\ q_e = log\ q_0 - K\ \epsilon^2 \quad \cdots\cdots\cdots\cdots\cdots(13)$$

Where q_0 represents the constant of D-R (mol/g), and K is the mean free energy of adsorption (kJ/mol). However, ϵ can be calculated using equation (14):

$$\epsilon = RT ln(1 + \frac{1}{C_e}) \quad \cdots\cdots\cdots\cdots\cdots\cdots (14)$$

Where C_e is the adsorbate equilibrium concentration, R is the ideal gas constant (8.314J/mol.K) and T is the temperature in Kelvin. The values of q_0 and K were calculated and tabulated in table (3) using slope and intercept from the plot of lnC_e against ϵ^2 respectively

From table 4, the isotherms data generated and reported were from three important isotherm models viz Langmuir, Freundlich and D-R models. The interpretation of the suitability of the isotherms model was decided only by linear regression coefficient (R^2) obtained for each model. The obtained values of R^2 suggested that the adsorption process at equilibrium was well fitted in the Freundlich isotherm compared to Langmuir and D-R model under a wide range of initial concentration. The applicability of the Freundlich isotherm indicates a multi-layer coverage with K_F values of 24.44mg/g adsorption capacity. While 1/n is the heterogeneity factor of adsorption obtained from slope of lnq_e against lnC_e. However, n value satisfies the condition of 1<n<10 which indicates favourable adsorption process [56].

Table 4. Adsorbent isotherm parameters for the adsorption of MG onto RWL adsorbent

Langmuir			
q_0 (mg/g)	K_L (L/mg)	R_L	R^2
909.10	0.026	0.242	0.9708
Freundlich			
1/n	n	K_F	R^2
1.088	0.920	24.44	0.9862
D-R Model			
q_0	β x10^{-6}	ϵ	R^2
242.82	2.0	0.246	0.9365

3.6 Thermodynamic Studies

The thermodynamic parameters give insight about the nature of adsorption process. The effect of temperature on the adsorption of MG onto RWL in aqueous media were studied by varying the temperature from 303 to 333K. The change of thermodynamics functions of adsorption such as Gibb's free energy (ΔG), Enthalpy (ΔH) and Entropy (ΔS) were generally obtained from equation (15) and (16) respectively.

$$\Delta G = -RT ln K_c \quad \cdots\cdots\cdots\cdots\cdots\cdots\cdots (15)$$

$$ln\ K_c = -\frac{\Delta G}{RT} = -\frac{\Delta H}{RT} + \frac{\Delta S}{R} \quad \cdots\cdots\cdots\cdots (16)$$

Where R is molar gas constant (8.314J/mol.K), T is absolute Temperature (K) and K_c is the thermodynamics equilibrium constant and was calculated from the relationship in equation (17) [57].

$$K_c = \frac{C_a}{C_e} \quad \cdots\cdots\cdots\cdots\cdots\cdots\cdots (17)$$

Where C_a is mg of MG adsorbed per litre, C_e is the equilibrium concentration of MG (mg/L).

Both ΔH and ΔS were calculated from slope and intercept of Van't Hoff plot in figure 7 of lnK_c versus $1/T$ using equation (16).

From table 5, the Gibb's free energy change of adsorption is negative indicating the spontaneity and feasibility of the adsorption process at all temperatures studied. The ΔH value was found to be -11.750kJ/mol which is less than 20kJ/mol and negative proved that the nature of the adsorption is physiosorption and exothermic respectively [58], while the negative value of ΔS indicates decrease in randomness in the adsorption process during the transfer of the molecules between the adsorbent and adsorbates [59-60].

Table 5: Thermodynamics parameters for the adsorption of MG onto RWL.

T(K)	ΔG (kJ/mol)	ΔH (kJ/mol)	ΔS(J/mol.K)
303	-9.707	-11.750	-6.330
313	-9.880		
323	-9.851		
333	-9.481		
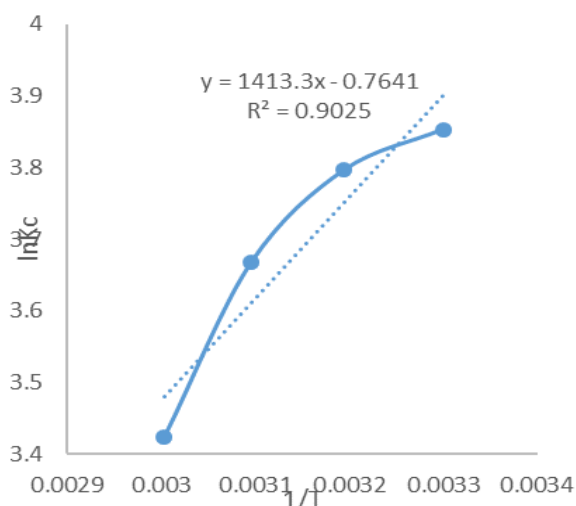
Fig 7. The Van't Hoff plot for Adsorption of MG onto RWL

3. Experimental

3.1 Sample collection and adsorbent preparation

The adsorbent was prepared according to method by Öznur *et al.* [25]. The water lily leaves (WLL) were obtained from Gubi Dam, Bauchi State, Nigeria. The leaves were washed thoroughly with distilled water to remove dust impurities and shade dried for 72hours. The dried leaves were ground to powder and sieved into a working size of 300μm and stored in an airtight container labelled as raw water lily (RWL) sample.

3.2 The physicochemical analysis of the adsorbents

Determination of ash and moisture content

The ash and moisture contents of RWL were determined by weight difference [26]. For moisture content, 1g of RWL was heated at 105°C for 3 hours, cooled in desiccator and re-weighed. The procedure was repeated several times at the same temperature for 15 min until constant weights were obtained. The percentage moisture content of the sample was determined using the equation (18):

$$Moisture\ content\ (\%) = \frac{w_1 - w_3}{w_2 - w_1} x\ 100 \quad ....(18)$$

Where, w_1 is weight of empty crucible, w_2 is weight of crucible and the sample before heating, w_3 final weight of the crucible and the sample after heating. In determination of ash content, 1g of RWL was placed in a crucible of known weight and then heated at 500^0C for 3 hours. The sample was cooled in desiccator and weighed. The ash content of each sample was calculated from the weight of the sample before and after heating using equation (19):

$$Ash\ content\ (\%) = \frac{w_1 - w_3}{w_2 - w_1} x\ 100 \quad ....\ (19):$$

Where, w_1 is the initial weight of crucible, w_2 is initial weight of the crucible and the sample before heating and w_3 is the final weight of sample and the crucible.

Determination of organic matter content

The organic matter contents of the adsorbents were determined from the difference between 100% air-dried adsorbent measured and the percentage ash content [20] as illustrated in equation (3):

$$OMC\ (\%) = 100 - \%Ash\ content \quad ....(20)$$

Determination of pH

1g of RWL sample was put inside a 250ml Erlenmeyer flask and 100ml of distilled water was poured into the flask. The solution was heated for 15minutes in a boiling condition. The solution was cooled at room temperature and dilute with distilled water to 100ml. the solution was stirred well and the pH was determined using pH meter [28].

Pore (Void) volume determination

In order to determine the pore volume of the adsorbent, method reported by Ayuba and Thomas [29] was adopted. 2.0g of the samples (RWL) was immersed in water and boiled for 15min. After the air in the pores had been displaced, the sample was then dried superficially and reweighed. The difference in weight divided by the density of water gave the pore volume as in equation (21):

$$Pore\ (void)volume = \frac{w_2 - w_1}{density\ of\ water} \quad ....(21)$$

Where, w_1 is the weight of empty density bottle and w_2 is the weight of density bottle and sample together, while the density of water is 1g/cm³

Bulk density (apparent density) determination

The bulk density of the sample was determined so as to know the packed density of a sample. Method reported by Giwa *et al.* [20] was adopted as in equation (22).

$$bulk\ density = \frac{\left(weight\ of\ the\ sample\ \left(\frac{g}{ml}\right)\right)}{100} \ \dots\dots.\ (22).$$

3.3 Determination of point of zero charge (PZC)

The pH drift method was adopted according to Nasiruddin and Sarwar [30]. The pH of 0.01 NaCl was adjusted to a value between 2 and 11 using 0.50M HCl or 0.50M NaOH. 0.10g RWL was added to the 50ml of the adjusted solution in a capped vial and equilibrated for 24hours. The final pH was measured and plotted against initial pH. The pH at which the curves intercepts the pH line was taking as point of zero charge.

3.4 FT-IR analysis

Fourier transform infrared spectroscopy was used to study the surface functional group of the adsorbent before and after the MG adsorption. IR spectra were obtained with a type spectrum 100 series FTIR spectrometer (Agilent Technology Perkin Elmer Spectrum 100, USA) using the transformation of 20 scans with spectral resolution of 4 cm^{-1} by attenuated total reflectance method. FTIR spectra were collected in the mid infrared region between 4,000 and 650 cm^{-1}. Spectra were acquired using air background correction [31].

3.5 Scanning electron microscope (SEM) analysis

Scanning electron microscope (SEM) analysis of surface morphology of the adsorbents was carried by viewing the electron micrographs of the materials [17]. Analysis was done with proxy Scanning Electron Microscope (phenom world Eindhoven). In sample preparation for the SEM analysis, a thin layer of adhesive serving as carbon glue was attached onto a stub, and very small amount of the materials to be view was spread on the stub materials and subsequently viewed in the instrument to obtain micrographs. Scanned micrographs of RWL before and after adsorption were taking at an accelerating voltage of 15.00kv and 1500X magnification respectively.

3.6 Preparation of stock solution

Stock solution of Malachite green dye (figure 8) were prepared by dissolving 1g of dye in 1000ml volumetric flask at room temperature and shaken until homogenous solution is obtained [32]. The sample of required concentration were prepared by diluting the stock solution with distilled water to a required concentration using dilution formula shown in equation (23).

$$C_1 V_1 = C_2 V_2 \ \dots\dots\dots\dots\dots\dots\ (23)$$

The concentration of residual un-adsorbed MG dye was measured at working wavelength (λmax = 615.50nm)

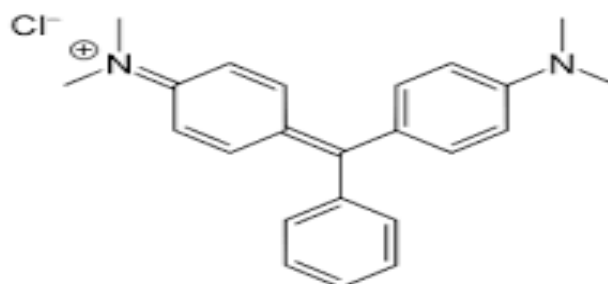using UV-visible spectrophotometer (Hitachi 2800 model).

Fig 8. Structure of Malachite Green.

3.7 Adsorption equilibrium experiments

For this experiment, the batch adsorption was adopted because of its simplicity [33]. The batch experiments were carried out to determine the optimum conditions for equilibrium adsorption of MG dye onto RWL adsorbent. The results obtained after optimization experiments (90min agitation period, 0.02g adsorbent dosage, 100ppm concentration, 11 pH of solutions) were used to conduct the batch adsorption experiments. This system was runs in a 60cm^3 polythene sample bottles at 30, 40, 50 and 60^{0}C temperature respectively. The samples were placed in temperature controlled shaker for the period reported. After reaching equilibrium period, the content was filtered and the filtrate was analysed using Perkin-Elemer UV-visible Spectrophotometer at maximum absorbance wavelength of 615.4nm. The amount of the adsorbed dye was obtained using equation (24):

$$q_e = \frac{(c_0 - c_e)}{m} x\ V \ \dots\dots\dots\dots\dots\ (24)$$

While colour removal rate (%Removal) was calculated using equation (25):

$$\%R = \frac{(c_0 - c_e)}{c_0} x\ 100 \dots\dots\dots\dots\dots..\ (25)$$

Where: q_e is adsorption capacity (mg/g), c_0 and c_e are the initial and final concentration in (mg/l) respectively for the dyes in the solution, V is the volume of the dyes in solution (L) and m is the mass of the adsorbents [32-33].

4. Conclusion

In conclusion, the RWL adsorbent were prepared from water lily leaves. It was characterized by determining its some physicochemical parameters and also using FT-IR and SEM techniques respectively. The prepared RWL has provide a significant adsorption capacity of 216.66mg/g of MG from aqueous solution due to high bulk density, porosity, and present of multifunctional groups. In addition, the adsorption data generated obeyed pseudo-second order kinetics and Freundlich isotherm models signifying exothermic, physiosorption and spontaneous nature of the adsorption process. Therefore, this cheap and efficient adsorbent can be utilized for effective removal of toxic and non-

biodegradable dyes such as malachite green from aqueous solution or dye contaminated industrial effluents.

References

[1] A. M. Ayuba, B. Idoko, Cowpea husk adsorbent for the removal of crystal violet dye from aqueous solution. *Arabian Journal of Chemical Research.* 8(1)(2021) 114-132.

[2] A. T. Khan, N. Momina, Enhanced adsorptive Removal of a mild acid dye Bromothymol blue from aqueous solution using magnetic chitosan-Bambo sawdust composite. Batch and Column Studies. *Environmental Progress & Sustainable Energy.* 5(34) (2015) DOI: 10.1002/ep

[3] H. Al-Aidy, E. Amdeha, Green adsorbent based on polyacrylic acid-acrylamide grafted starch hydrogels: the new approach for enhanced adsorption of malachite green dye from aqueous solution. *International Journal of environmental analytical chemistry,* (2020) ISSN: 0306-7319.

[4] M. Wu, S. Zhao, R. Jing, Y. Shao, X. Liu, L. Fengzhu, X. Hu, Q. Zhang, Z. Meng, A. Liu, Competitive adsorption of anti-biotic tetracycline and Ciprofloxacin on montmorillonite. *Journal of applied clay Sciences,* 180 (2019) 105175.

[5] M. Rajabi, K. Mahanppor, O. Moradi, Preparation of PMMA/GO and PMMA/GO-Fe2O3 nanocomposite for Malachite Green dye adsorption: kinetics and Thermodynamics Studies. *Composite part B: Engineering,* 167 (2019) 544-555.

[6] G. Crini, H. N. Peindy, F. Gimbert, C. Robert, Removal of Malachite Green from aqueous solution by adsorption using cyclodextrin-based adsorbent: kinetic and Equilibrium studies. *Journal of separation and Purification Technology,* 53(1) (2017) 97-110.

[7] W. T. Tsai, H. R. Chen, Removal of Malachite Green from aqueous solution using low-cost chlorella-based biomass. *Journal of Hazardous Materials,* 175(1-3) (2010) 844-849.

[8] P. Saha, S. Chowdbury, S. Gupta, I. Kumar, R. Kumar, Assessment On the Removal of Malachite Green Using Tamarind Fruit Shell as Adsorbents. *Clean Soil Air Water,* 38 (2010) 437-445.

[9] S. Chowdbury, P. Saha, Shea Shell Powder as a New Adsorbent to Remove Basic Green 4 (Malachite Green) From Aqueous Solutions: Equilibrium, Kinetics and Thermodynamics Studies. *Chemical Engineering Journal,* 164 (2010) 168-177.

[10] S. Ullah, A. Ur Rahman, F. Ullah, A. Rashid, T. Arshad, E. Viglasova, M. Galambos, M. N. Mahmoode, H. Ullah, Adsorption of Malachite green dye onto mesoporous natural inorganics clays: equilibrium isotherm and kinetic studies. *Water,* 13 (2021) 965.

[11] J. Zhang, L. Wang, G. Zhang, Z. Wang, L. Xu, Z. Fan, Influence of azo dye-TiO$_2$ interaction on the filtration performance in a hybrid photocatalysis/ultrafiltration process. *Journal of Colloid interface sciences,* 389 (2013) 273-283.

[12] H. El-Boujaady, M. Mourabet, H. Bennani-Ziatni, A. Taitai, Adsorption/Desorption of Direct yellow 28 on apatitc phosphate: mechanism, Kinetics and Thermodynamics. *Journal of the Association of Arabs Universities for basic and applied sciences* 16 (2014) 64-73.

[13] N. M. Maezawa, H. Nakadoi, K. Suzuki, T. Furusawa, Y. Suzuki, S. Uchida, Treatment of dye wastewater by using photocalytic oxidation with sonification. *Ultrasonic sonochemistry,* 14(5) (2007) 615-620.

[14] M. Aazza, H. Moussout, R. Marzouk, H. Ahlafi, Kinetic & thermodynamics studies of malachite green adsorption on alumina. *Journal of Materials and Environmental Sciences,* 8(8) (2017), ISSN: 2028-2508, pp 2694-2703.

[15] S. Jayanthi, N. K. Eswar, S. A. Singh, K. Chatterjee, G. Madras, A. Sood, Macroporous Three Dimensional Graphene Oxides Foams for Dyes Adsorption and Antibacterial Applications. *Royal Society Chemistry Advances,* 6 (2016) 1231-1242.

[16] S. Bentahar, A. Dbiki, M. El-Khomri, N. El-Messaoudi, A. Lacherai, Adsorption of Methylene Blue, Crystal Violet and Congo Red from Binary and Ternary Systems with Natural Clay: Kinetics, Isotherms and Thermodynamics. *Journal of Environmental Chemical Engineering,* 5 (2017) 5921-5932.

[17] S. A. Sartape, M. A. Mandhare, V. V. Jadhav, D. P. Raut, A. M. Anusa, S. S. Kolekar, Removal of malachite green dye from aqueous solution with sorption techniques using Limonia Acidissima (wood apple) Shell as low cost adsorbents. *Arabian Journal of Chemistry,* 10 (2017) 3229-3238.

[18] B. H. Hameed, M. I. El-khaiary, Malachite green adsorption by rattan sawdust: Isotherms, Kinetics and Mechanism Modelling. *Journal of hazardous Materials,* 159 (2008) 574.

[19] E. Sebata, M. Moyo, U. Guyo, N. P. Ngano, B. C. Nyamunda, F. Chigondo, M. S. Chitsa, Adsorptive Removal of atrazine from aqueous solutions using Bambara Groundnut hulls. *International Journal of Engineering research and Technology,* 2(5) (2013) 312-321.

[20] S. O. Giwa, J. S. Moses, A. A. Adeyi, A. Giwa, Adsorption of Atrazzine from aqueous solution using Desert Date Seed Shell activated Carbon. ABUAD *Journal of Engineering Research & Development (AJERD),* 1(3) (2018) 317-325.

[21] D. Prahas, Y. Kartika, N. Indraswati, S. Ismadji, Activated carbon from jackfruit peel waste by H$_3$PO$_4$ chemical activation: pore structures and surface chemistry characterization. *Chemical Engineering Journal,* 140 (2008) 32-42.

[22] C. C. O. Alves, A. S. Franca, L. S. Oliviera, Evaluation of an adsorbent based on agricultural waste (corn cob) for removal of Tyrosine and Phenylamine from aqueous solutions. *Biomedical Research Journal International* (2013) 1-5.

[23] T. Nharingo, N. M. Muzondo, E. Madungwe, F. Chigondo, U. Guyo, B. Nyumunda, Isotherm studies of the biosorption of Cu(II) from aqueous solution by vigna subterranean (L) Verdc hull. *International Journal of*

Scientific Research and Technology, 2(4) (2013) 199-206.

[24] A. D. N'diaye, M. Sid', M. Konkou Adsorption of Aspirin onto Biomaterials from aqueous solutions. *Journal of materials and Environmental Sciences*, 11 (2020) 1839-1845.

[25] D. Oznur, I. Fatma, T. Kadir, O. Mahmure, Sumec leaves as a Novel low cost adsorbent for removal of basic dyes from aqueous solution. *Hindawi publishing corporation (ISRN) analytical Chemistry volume* (2013). Article ID. 1210470, 9 pages.

[26] U. I. Gaya, E. Otene, A. H. Abdullahi, Adsorption of aqueous Cd (II) and Pb(II) on activated carbon nanopores prepared by chemical activation of doum palm shell. *SpringerPlus* 4 (2015) 458.

[27] M. B. Ibrahim, M. S. Sulaiman, S. Sani, Assessment of adsorption properties of neem leaves waste for the removal of congo red and methylene orange. *3rdn international conference on biological, chemical and environmental sciences* (BCES-2015) September 21-22, Kuala Lampur, Malaysia (2015).

[28] O. J. Amode, H. J. Santos, M. Z. Alam, H. A. Mirza, C. C. Mei, Adsorption of methylene Blue from aqueous solution using untreated and treated (*Metroxylon spp*) wate adsorbents: equilibrium and Kinetic studies. *International Journal of Industrial Chemistry* 7 (2016) 333-345.

[29] A. M. Ayuba, N. A. Thomas, Paraquat dichloride adsorption from aqueous solution using carbonised Bambara groundnut (vigra subterranean) shells. *Bayero journal of pure and applied sciences,* 12(1) (2019) 167-177. ISSN 2006-6996.

[30] K. M. Nasiruddin, A. Sawar, Determination of point of zero charge of natural and treated adsorbents. *Surface review and letters,*14, 3(2007) 461-469.

[31] S. M. Anisuzzaman, G. C. Joseph, A. M. S. B. W. Daud, D. Krishnaiah, H. S. Yee, Preparation and characterization of activated carbon from typha orientalis leaves. *International Journal of Industrial Chemistry*, 6 (2014) 9-21.

[32] M. B. Ibrahim, S. Sani, Neem (Azadirachta Indica) leaves for the removal of organic pollutants. *Journal of geosciences and environmental protection*, 3 (2015) 1-9.

[33] Z. Shahryari, S. A. Goharrizi, M. Azadi, Experimental study of methylene blue adsorption from aqueous solution onto a carbon nanotube. *International Journal of water Resources and environmental engineering,* 2(2) (2010) 016-028.

[34] S. O. Bello, A. K. Adegoke, O. O. Akinyinni, Preparation and characterization of novel adsorbents from *Moringa Oleifera* leaf. *Appl. Water Sci.* 7 (2017) 1295-1305. DOI: 10.1007/s13201-05-0345-4.

[35] A. Zulkania, H. F. Ghina, S. R. Amelia, The potential of activated carbon derived from bio-char pyrolysis as adsorbents. *MATEC Web of Conferences* 154 (2018), 01029. ICET4SD 2017.

[36] P. Ravichandran, P. Sugumaran, S. Seshadri, Preparation and Characterization of activated carbon derived from palmyra wastes coastal region. Preceding of international Conferences on "impact of Climate Change on Coastal Ecosystem" (ICC-ECO 2011). Athyabama University, Jappiar Nagar, Chennai, India (2011).

[37] B. A. Karim, B. Mounir, M. Hachkar, M. Bakasse, A. Yaacoubi, Adsorption/Desorption behaviour of cationic dyes on Moroccan Clay: equilibrium & Mechanism. *Journal of Materials and Environmental Sciences*. 8(3) (2017) 1082-1096.

[38] P. K. Parhi, B. K. Bindhari, R. K. Mohapatra, S. Das, S. S. Behera, B. M. Murmur, Extensive Investigation on the study for the adsorption of Bromocresol Green (BCG) dye using activated phragmites karka. *Indian Journal of Chemical Technology,* 25 (2018) 409-420.

[39] K. A. G. Gusmao, L. V. A. Gurgel, T. M. S. Melo, L. F. Gil, Adsorption Studies of Methylene Blue and Gentian Violet On Sugarcane Bagasse Modified with EDTA Dihydride (EDTAD) In Aqueous Solutions: Kinetics & Equilibrium Aspects. *Journal of Environmental Management,* 118 (2013) 681-689.

[40] L. K. Akinlola, A, M. Umar, Adsorption of Crystal Violet onto Adsorbents Derived from Agricultural Waste: Kinetics and Equilibrium Studies. *Journal of Applied Science and Environmental Management,* 19(2) (2015) 279-288.

[41] J. Zhang, L. Wang, G. Zhang, Z. Wang, L. Xu, Z. Fan, Influence of azo dye-TiO$_2$ interaction on the filtration performance in a hybrid photocatalysis/ultrafiltration process. *Journal of Colloid interface sciences*, 389 (2013) 273-283.

[42] M. A. Bedmohata, A. R. Chaudhari, S. P. Singh, M. D. Choudhary, Adsorption capacity of activated carbon prepared by chemical activation of Lignin for the removal of methylene blue dye. *International Journal of advanced Research in Chemical Science (IJARCS),* 2(8) (2015) 1-13.

[43] X. Liu, F. Yan, Y. Wang, Q. Gau, S. Ren, Y. Wen, B. Shen, Synthesis and Characterization of Multi-Active Site Grafting Starch Copolymer Initiated by KMNO$_4$ and HIO$_4$/H$_2$SO$_4$ Systems. *Journal of Carbohydrate Polymers,* 117 (2015) 247-254.

[44] S. A. Yusuff, Adsorption of Hexavalent Chromium from Aqueous Solution by *Leucaena Leucocephala* Seed Pod Activated Carbon: Equilibrium, Kinetics and Thermodynamics Studies. *Arab Journal of Basic and Applied Sciences* (2019) DOI: 10.1080/25765299.2019.1567656.

[45] K. C. Enenebeaku, J. N. Okorocha, E. U. Enenebeaku, I. J. Okolie, B. Anukum, Adsorption of malachite green from aqueous solution by PNSBP: equilibrium, kinetic and thermodynamics studies. *IOSR Journal of applied Chemistry*, 9 (9) (2016) e-ISSN: 2278-5736, 28-38.

[46] N. Abdul-salam, S. K. Adekola, Adsorption studies of Zinc (II) on magnetite, baobab (*Adensonia digitate*) and magnetite-baobab composite. *Journal of applied water Sciences,* 8 (2018) 222.

[47] X. Han, J. Yuan, X. Ma, Adsorption of Malachite Green from aqueous solutions onto lotus leaf: Equilibrium, Kinetics and Thermodynamics Studies. *Desalination and water Treatment*, 52(2) (2013) 5563-5574.

[48] D. Pathania, S. Sharma, P. Singh, Removal of methylene blue by adsorption onto activated carbon developed from *Ficus carica bast. Arabian Journal of Chemistry* (2017) DOI: 10.1016/j-arabjc.2013.04.021.

[49] Y. Al-degs, M. A. M. KHraisheh, S. J. Allen, M. N. Ahmad, G. M. Walker, Competitive adsorption of reactive dyes from solution: equilibrium isotherm studies

in single and multisolute systems. *Chemical Engineering Journal*, 128 (2007) 163.

[50] M. Aazza, H. Moussout, R. Marzouk, H. Ahlafi, Kinetic & thermodynamics studies of malachite green adsorption on alumina. *Journal of Materials and Environmental Sciences*, 8(8) (2017), ISSN: 2028-2508, 2694-2703.

[51] X. Pan, D. Zhang, Removal of malachite green from water by firmiana simplex wood fiber, *e-Journal of biotechnology,* 12(4) (2009) ISSN: 0177-3458.

[52] L. R. Bonetto, F. Ferarini, C. DeMarco, J. S. Crespo, R. Guegun, M. Giovanela, Removal of Methyl violet 2B dye from aqueous solution using a magnetic composite as adsorbent. *Journal of water process Engineering*, 6 (2015)11-20.

[53] H. Khawaja, E. Zahir, M. Asif Asghar, M., Arif Asghar, Graphene oxide decorated with Cellulose and Copper nanoparticles as an efficient adsorbent the removal of malachite green. *International Journal of Biological molecules,* 167 (2021) 23-34.

[54] M. H. Dehgani, S. Tajik, A. Panahi, M. Khezri, A. Zarei, A. Heidarinejad, M. Yousefi, Adsorptive removal of noxious cadmium from aqueous solution using polyureaformaldehyde: a novel polymer adsorbent. *MethodsX,* 5 (2018) 1148-1155.

[55] I. Nica, C. Zaharia, R. I. Baron, S. Coseri, D. Suteu, Adsorptive materials based on preparation, characterization and application of copper ion retention. *Cellulose Chemistry Technology,* 54(5-6) (2020) 579-590.

[56] A. G. Farombi, O. S. Amuda, M. M. Raimi, A. O. Olayiwola, Studies on Naphthalene adsorption from contaminated water using hydroxyapatite produced from catfish bones. *FUTA Journal of Research in sciences,* 15(01) (2019) 150-163.

[57] N. Hassan, A. Shahat, A. El-Didamony, M. G. El-Desouky, A. A. El-Bindary, Equilibrium, Kinetic and Thermodynamics Studies of adsorption of cationic dyes from aqueous solution using ZIF-8. *Molecular Journal of Chemistry,* 8(3) (2020) 627-637.

[58] N. Wibowo, L. Setiyadhi, D. Wibowo, J. Setiawan, S. Ismadji, Adsorption of Benzene & Toluene from Aqueous Solution onto Activated Carbon and Its Acid & Treated Forms: Influence of Surface Chemistry On Adsorption. *Journal of Hazardous Materials,* 146 (2017) 237-242.

[59] M. K. Dahri, M. R. R. Kooh, L. B. Lim, Water remediation using low cost adsorbent walnut shell for removal of malachite green: equilibrium, kinetics, thermodynamics and regeneration studies. *Journal of environmental chemical engineering,* 2(3) (2014) 1434-1444.

[60] A. Machrouhi, M. Farnane, A. Elhalil, M. Abdennouri, H. Tounsadi, N. Barka, Heavy metals biosorption by *thapsiantran stagana* stems powder: Kinetics, equilibrium and thermodynamics. *Molecular Journal of Chemistry,* 7(1) (2019) 098-110.